Rheokinetics of graft copolymerization of acrylamide in concentrated starch and rheological behaviors and microstructures of reaction products

Xianyang Bao[a,b,c], Long Yu[a,d,*], George P. Simon[b], Shirley Shen[c], Fengwei Xie[e,f,g,†], Hongsheng Liu[a,d], Ling Chen[a], Lei Zhong[h]

[a] *Center for Polymer from Renewable Resources, SFSE, South China University of Technology, Guangzhou, Guangdong 510640, China*

[b] *Department of Materials Science and Engineering, Monash University, Melbourne, Vic 3800, Australia*

[c] *CSIRO Manufacturing, Bayview Avenue, Clayton, Vic 3168, Australia*

[d] *Sino-Singapore International Joint Research Institute, Guangzhou, Guangdong 510663, China*

[e] *Institute of Advanced Study, University of Warwick, Coventry CV4 7HS, United Kingdom*

[f] *International Institute for Nanocomposites Manufacturing (IINM), WMG, University of Warwick, Coventry CV4 7AL, United Kingdom*

[g] *School of Chemical Engineering, The University of Queensland, Brisbane, Qld 4072, Australia*

[h] *School of Chemistry and Chemical Engineering, Guangxi Key Laboratory Cultivation Base for Polysaccharide Materials and Modifications, Guangxi University for Nationalities, Nanning, Guangxi, China*

[*] Corresponding author. Email: felyu@scut.edu.cn (L. Yu)

[†] Corresponding author. Email: f.xie@uq.edu.au, fwhsieh@gmail.com (F. Xie)

Abstract:

A widely recognized challenge in starch chemistry is to manipulate the graft copolymerization onto starch melt by reactive extrusion (REX). To understand the complex *in-situ* graft copolymerization in highly concentrated systems, we firstly used a mixer to achieve a homogeneous viscous starch melt, and then undertook dynamic rheological measurements to study the rheokinetics of the reaction. The *in-situ* synthesis also facilitated the characterization of the microstructures of reaction products. The melt mixture could be regarded to be completely micromixed since the rheokinetics was predominated by the reaction kinetics. The rheological characterization revealed that G' of hydrogels followed a linear progression with the crosslinker concentration. Nevertheless, the reaction temperature and initiator content had little influence on the final microstructure of hydrogels, most likely due to the strong chain transfer reaction in the melt. Additionally, high-amylose starches tended to form grafted hydrogels with a high physical crosslinking density.

Keywords: starch; acrylamide; hydrogel; graft copolymerization; kinetics; rheology

Chemical compounds studied in this article:

Starch (PubChem CID: 24836924); Acrylamide (PubChem CID: 6579); Ammonium persulfate (PubChem CID: 62648); *N*,*N'*-Methylenebisacrylamide (PubChem CID: 8041); Water (PubChem CID: 962)

1. Introduction

Hydrogels are 3D matrices constituted by linear or branched hydrophilic polymers that are chemically or physically crosslinked (Ahmed, 2015; Ullah, Othman, Javed, Ahmad, & Akil, 2015). Hydrogels have been widely applied in various fields such as medicines (Khalid, Ahmad, Minhas, & Barkat, 2017; Lam et al., 2016), engineering (Dai et al., 2017; Mohammadi, Sun, Berkland, & Liang, 2017), and agriculture (Bao et al., 2015; Elbarbary, El-Rehim, El-Sawy, Hegazy, & Soliman, 2017), due to their 3D network and unique properties. In agriculture, the hydrogels have been adopted to modify the soil environment and enhance the utilization efficiency of water and fertilizers, which contributes to the growth of crops and alleviates the damage to the environment from the leaching loss of fertilizers (Guilherme et al., 2015; Zhang et al., 2017b). Moreover, encapsulation with hydrogels has been proved useful for the controlled release of pesticides for sustainable agriculture (Sarkar & Singh, 2017; Sun, Ma, Fang, Ren, & Fu, 2016). However, traditionally synthesized polymers are not biodegradable, which restricts their industrial application in agriculture. Therefore, natural polysaccharides such as cellulose (Ibrahim, Abd‐Eladl, & Abou‐Baker, 2015; Zhang et al., 2017a), lignocellulose (El-Saied, Waly, & Basta, 2000; El-Saied, Waley, Basta, & El-Hadi, 2004; El-Saied, Basta, El-Hadi, & Waley, 2007), starch (Qiao et al., 2016; Singh, Sharma, Negi, & Dhiman, 2015), and chitosan (Kashyap, Xiang, & Heiden, 2015; Perez & Francois, 2016) have been studied for the synthesis of hydrogels, due to their abundance, biodegradability, renewability, and low cost. Starch is one of the first and most promising materials used to produce hydrogels due to its chemical versatility and relatively easier processability among polysaccharides (Ismail, Irani, & Ahmad, 2013; Zhang & Xu, 2017). Polysaccharide-based hydrogels are traditionally fabricated using batch processing methods such as solution, emulsion, and inverse suspension polymerization. However, these batch-processing methods are usually solvent-intensive, have low efficiency, and tend to generate significant amounts of byproducts, which have greatly

restricted their industrial applications (Moad, 2011; Xie, Yu, Liu, & Chen, 2006).

During the past decades, continuous reactive extrusion (REX) has emerged as a solvent-free, cost-effective, and environmentally friendly technology to produce new materials with desired properties and added functions. Based on these advantages, REX has been introduced to the chemical processing of bio-based polymeric materials to tailor their properties, which has been known as *in-situ* REX (Formela, Hejna, Haponiuk, & Tercjak, 2017). Recently, *in-situ* REX has been successfully applied into the chemical modification, compatibilization, and functionalization of the bio-based polymers, such as polylactide (PLA) (Ojijo & Ray, 2015; Yang, Clénet, Xu, Odelius, & Hakkarainen, 2015), cellulose (Wei, McDonald, & Stark, 2015; Zhang, Li, Li, Gibril, & Yu, 2014), starch (Willett & Finkenstadt, 2015; Xu et al., 2017), lignin (Luo, Cao, & McDonald, 2016), and polycaprolactone (PCL) (Cayuela, Da Cruz-Boisson, Michel, Cassagnau, & Bounor-Legaré, 2016; Garcia-Garcia, Rayón, Carbonell-Verdu, Lopez-Martinez, & Balart, 2017). The main advantages of *in-situ* REX are the reduced costs due to a combination of polymer melting, physical blending of mixtures, and chemical reaction without purification of the final products.

It is well known that the high viscosity of polymer melt, the high shear stress involved in extrusion, and the complicated reactions between the used components, make it difficult to control the REX process precisely. All of these effects make a difference through the viscoelastic behaviors of reactive melt, which are always involved in the structural evolution during the reaction. In particular, polymer melts are usually viscoelastic and exhibit temperature-dependence and shear-dependence (non-Newtonian behavior). Therefore, the rheological behaviors of polymer melts during the REX process, known as rheokinetics, become essential in modeling REX and optimizing variable processing conditions.

Traditionally, a static mixer (torque rheometer) with a torque that is monitored has usually been

used to study the rheokinetics of reaction systems with high viscosities. In particular, for polymer melts, the reaction between the polymer chains is usually controlled by the diffusion rate of mass transfer rather than the kinetics of chemical bonding mechanisms (Witono, Noordergraaf, Heeres, & Janssen, 2017; Zhou, Yu, & Zhou, 2009). However, a static mixer may not be suitable for studying all the reactions. For example, when crosslinking is involved to form a heterogeneous network, the shear stress during mixing breaks the newly formed network into large amounts of microgels due to the stress concentration effect (Cicuta & Donald, 2007; Waigh, 2016). These microgels, which are more likely to form *in-situ*, could slip between each other and thus their true viscoelasticity could not be reflected in the torque rheometer.

To address the above-mentioned issue, we utilized the graft copolymerization of acrylamide (AM) onto starch melt as the model reaction to develop a new method to study the reaction rheokinetics to guide the REX of concentrated polysaccharide systems. In this method, a modified Haake mixer was used to gelatinize and homogenize concentrated starch with the addition of required reactants, which could be regarded as *completely micromixed* to ensure a sufficient and free selectivity between the reactive groups. Then, an *in-situ* synthesis was performed in a stress-controlled rheometer through dynamic shear oscillation to study the reaction rheokinetics of starch graft copolymerization. Furthermore, the *in-situ* synthesis in a rheometer provides an incomparable benefit to allow investigating the microstructures of intact hydrogel after the chemical reaction is complete. In this way, the relationship between the reaction conditions, the graft polymerization rheokinetics, and the microstructure of the 3D network of starch-*g*-PAM hydrogels could be established for the first time.

In previous studies of the graft copolymerization of concentrated starch by REX (Carr, Kim, Yoon, & Stanley, 1992; Finkenstadt & Willett, 2005; Willett & Finkenstadt, 2003, 2006a, b, 2009; Willett & Finkenstadt, 2015; Yoon, Carr, & Bagley, 1992), different reaction parameters such as the types of

starch and monomer, moisture content, starch-to-monomer ratio, reaction temperature, content and type of the initiator, degree of filling, and extruder screw speed on the graft parameters of grafted starch have been fully investigated. Therefore, the effects of this wide range of reaction parameters were not the focus in this current work but we only investigated the parameters that would directly influence the reaction kinetics, microstructures, and rheological properties of the hydrogels, including the contents of the crosslinker and the initiator and the reaction temperature. Nonetheless, we used corn starches with different amylose/amylopectin ratios as model materials to further explore the effect of molecular structure on the rheokinetics of starch graft copolymerization and the microstructures of final products. As much work has been undertaken to understand the *in-situ* REX for starch-*graft*-polyacrylamide (starch-*g*-PAM), the results from this work could be compared with the previously published results to validate the feasibility of our methodology.

2. Materials and Methods

2.1. Materials

Corn starches with different amylose/amylopectin ratios were used. Waxy corn starch (WCS) (amylose/amylopectin ratios: 0/100) and normal corn starch (NCS) (amylose/amylopectin ratios: 27/73) were purchased from Zhongliang Co., Ltd. Gelose 50 (G50) (amylose/amylopectin ratios: 50/50) and Gelose 80 (G80) (amylose/amylopectin ratios: 80/20) were acquired from Penford (Australia).

Acrylamide (AM) and *N,N'*-methylene-bisacrylamide (MBA) were purchased from Tianjin Kermel Chemical Reagent Co., Ltd. (China); and ammonium persulfate (APS) from Sinopharm Chemical Reagent Co., Ltd. (China). All chemicals were of analytical grade and used without further purification.

2.2. Preparation of reactive mixtures

A mixing system was established based on a modified Haake Rheomix 600p twin-rotor mixer

(Thermo Haake, Germany), which can provide high torque for the processing of highly viscous materials. One of the key requirements was to seal the mixer since the blending of the reactive mixtures needed to be carried out with water. The details of the modification of the mixer have been described previously (Xiao et al., 2017).

To ensure a high graft efficiency and monomer conversion in the experiment, we used optimized experimental conditions and procedures for the starch graft copolymerization, that is, the use of the initiator APS, the simultaneous initiation, and a high ratio of starch to monomer. The choice of such conditions and procedures is based on the literature. Specifically, compared with other initiators, the initiator APS could give a higher monomer conversion (Willett & Finkenstadt, 2006a). Besides, the graft efficiency decreased with the increasing ratio of acrylamide to starch (Finkenstadt & Willett, 2005). Moreover, in a concentrated system, there would be a greater possibility of chains transfer reaction, which competes with the homopolymerization (Willett & Finkenstadt, 2009). The simultaneous initiation rather than a pre-initiation process could ensure a high grafting efficiency because the completed micromixing of reactant mixtures is a prerequisite for a high reaction efficiency in the melted system (Janssen, 2004).

The reactive mixture was firstly prepared by mixing 20.0 g of starch, 10.0 g of AM, certain amounts of MBA, and 45.0 g of distilled water in the mixing chamber at 80 °C and 80 rpm, maintained for 5 min to gelatinize the starch under shear stress. Following this, the temperature of the mixer was reduced to 30 °C using compressed air, and 5 mL of a freshly prepared APS solution was added with a mixing speed of 100 rpm for 2 min to obtain a homogeneous reactive mixture. The ratio of starch to AM (w/w) we used was 2:1, which could give a high monomer conversion (90.4%) and grafting efficiency (79.0%) for the starch graft copolymerization (Finkenstadt & Willett, 2005). The FTIR spectra in **Fig. S1** indicated that the AM was grafted onto the starch successfully.

157

158 *2.3. Rheological measurements*

159 The graft copolymerization process of the starch was monitored using a stress-controlled Discovery
160 Hybrid Rheometer (TA Instruments, New Castle, DE 19720, USA) equipped with a Peltier device for
161 the temperature control. A stainless-steel parallel-plate geometry with a diameter of 20 mm was used to
162 perform the oscillatory measurements. During such measurements, a solvent trap and coating with
163 silicone oil around the edge of the samples was used to minimize water evaporation. The premixed
164 mixture was loaded onto the lower plate of the rheometer with a pre-setting temperature of 20 °C since
165 this temperature was low enough to prevent a further chemical reaction. The upper plate was set at a
166 desired gap from the bottom plate (500 μm), and this gap was thin enough to quickly reach temperature
167 equilibrium (no more than 1 min). An angular frequency of ω = 1 rad/s and a strain of γ = 0.5% were
168 selected to ensure deformation in the linear elastic regime at the required conditions. During reaction
169 monitoring process, the elastic modulus G' and the viscous modulus G'' were recorded every 30 s.

170 Once the graft polymerization was complete (within 50 minutes), a dynamic frequency sweep test
171 ranging from 0.1 to 100 rad/s was performed with a strain of γ = 0.5% at 25 °C. The
172 temperature-dependence behaviors of elastic modulus G' of the hydrogels were determined using
173 constant oscillatory strain and frequency (γ = 0.5% and ω = 1 rad/s) for a temperature sweep from 10 to
174 60 °C at 5 °C/step, allowing 2 min of temperature equilibrium before each measurement for every point.
175 To identify the linear viscoelastic region and characterize the microstructure of samples, the strain
176 sweep was also carried out under the conditions of ω = 10 rad/s and T = 60 °C.

177 For all the reported results, average and standard deviations were calculated from triplicate
178 measurements.

179

3. Results and discussion

3.1. Effect of crosslinker concentration (%C)

The amount of crosslinker for the graft copolymerization reaction could strongly influence the 3D network architecture of the resultant hydrogels. **Fig. 1** shows variations in the elastic modulus $G'(t)$ (a) and the viscous modulus $G''(t)$ (b) during the starch graft copolymerization with different MBA contents (*%C*). *%C* represents the molar fraction of the MBA crosslinker relative to the AM monomer. After a short induction period, when the elastic moduli remained stable, both G' and G'' then increased monotonically for all the samples and subsequently reached a plateau. Some scattering could be observed for $G''(t)$, due to the sensitivity of rheometer and the properties of crosslinking network ($G' \gg G''$) (Calvet, Wong, & Giasson, 2004). When $G'(t)$ and $G''(t)$ reached plateaus, it could be indicated that the graft polymerization was complete.

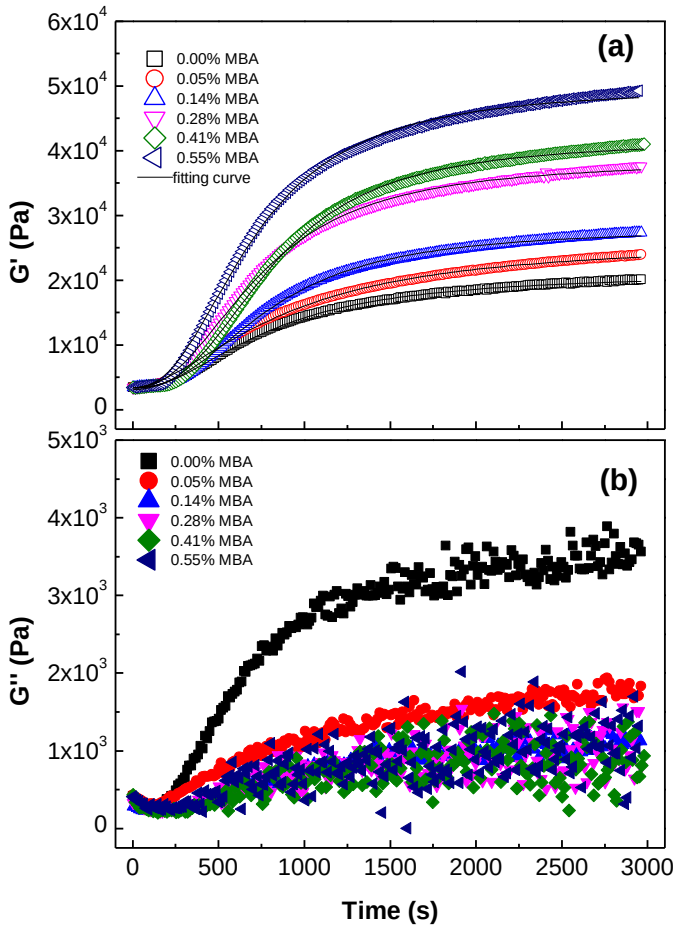

Fig. 1. Variations in (a) elastic moduli *G'* and (b) viscous moduli *G''* during graft copolymerization of NCS with 0.36% initiator (*%I*) and different crosslinker concentrations (*%C*). All measurements were performed at 60 °C under dynamic oscillations at γ = 0.5% and ω = 1 rad/s. The solid lines in (a) represent fitting curves using modified Hill equation (Equation 1).

To quantitatively analyze the rheokinetics of the starch graft copolymerization under different reaction conditions, the curves of elastic moduli $G'(t)$ were fitted with a modified Hill equation (Calvet et al., 2004; Giraldo, Vivas, Vila, & Badia, 2002):

$$G'(t) = G'_0 + (G'_\infty - G'_0)\frac{t^n}{t^n + \theta^n} \quad (1)$$

where G'_0 is the initial elastic modulus of reactive mixture, and G'_∞ corresponds to the final steady state elastic modulus. The half gelation time θ is the time for which $G'(\theta) = (G'_\infty - G'_0)/2$, and *n* is a coefficient related to the asymptotic slop *P* at the half gelation time θ with

$$P = \frac{n(G'_\infty - G'_0)}{4\theta} \quad (2)$$

Equation 2 can be used to characterize the gelation rate of starch copolymerization. The values of steady-state elastic modulus G'_∞, half gelation time θ, coefficient *n* and gelation rate *P* obtained from the fitting are shown in **Table S1**. Both G'_∞ and *P* increased linearly with *%C* with fitting curves listed in **Table S1**. However, *%C* did not influence the value of θ, which was 791 ±44 s, with *n* kept at 2.17 ± 0.30.

Once the graft polymerization was complete, dynamic oscillatory measurements at different frequencies, temperatures, and strains were performed to characterize the microstructures of grafted starch hydrogels. **Fig. 2a** shows the variations in $G'(\omega)$ and $G''(\omega)$ as a function of frequency using $\gamma = 0.5\%$ and $T = 25$ ℃. The frequency-dependence of $G'(\omega)$ and $G''(\omega)$ for the gels is usually expressed as a power-law behavior: (Madbouly & Otaigbe, 2005; Winter & Chambon, 1986)

$$G' \sim \omega^{n'} \ \& \ G'' \sim \omega^{n''} \quad (3)$$

The exponent n' and n'' which are fitting slops from the log-log plots of G' and G'' versus ω respectively, are called the relaxation exponent and can be linked to the material microstructure. Both

G' and G'' for all the samples increased slightly with the rise in frequency from 0.1 to 100 rad/s in **Fig. 2a**. The grafted starch hydrogels with a higher concentration of the crosslinker showed a weaker frequency-dependence for G' (smaller n') and stronger for G'' (larger n''). With an increase in the crosslinker content, G' of the hydrogels became increasingly independent of frequency over at least three decades, which was a characteristic of a well-developed 3D structure of the chemically crosslinked hydrogels (Madbouly & Otaigbe, 2005; Takenaka, Kobayashi, Hashimoto, & Takahashi, 2002). **Fig. 2b** shows the temperature-dependence of G' for the hydrogels with different crosslinker contents, with the temperature swept from 10 to 60 °C. For the more rigid hydrogels ($C\% > 0.05\%$), G' initially increased, showing its maxima at a certain temperature T_{max}, and then decreased. However, for the softer hydrogels ($C\% < 0.14\%$), G' decreased all along as the temperature increased. Furthermore, a higher crosslinker concentration in the hydrogels corresponded to a greater T_{max} for the rigid gels and a slower decay rate for the soft gels. The linear viscoelastic region of hydrogels is also shown in **Fig. 2c**, from which it is clear that $\gamma = 0.5\%$ used in the experiments here was within the linear viscoelastic domain. Moreover, with the increased crosslinker content, the critical strain after the linear domain of samples was reduced, which could be attributed to the increase of formation of chemically crosslinked points and the decrease in the mesh size of the network.

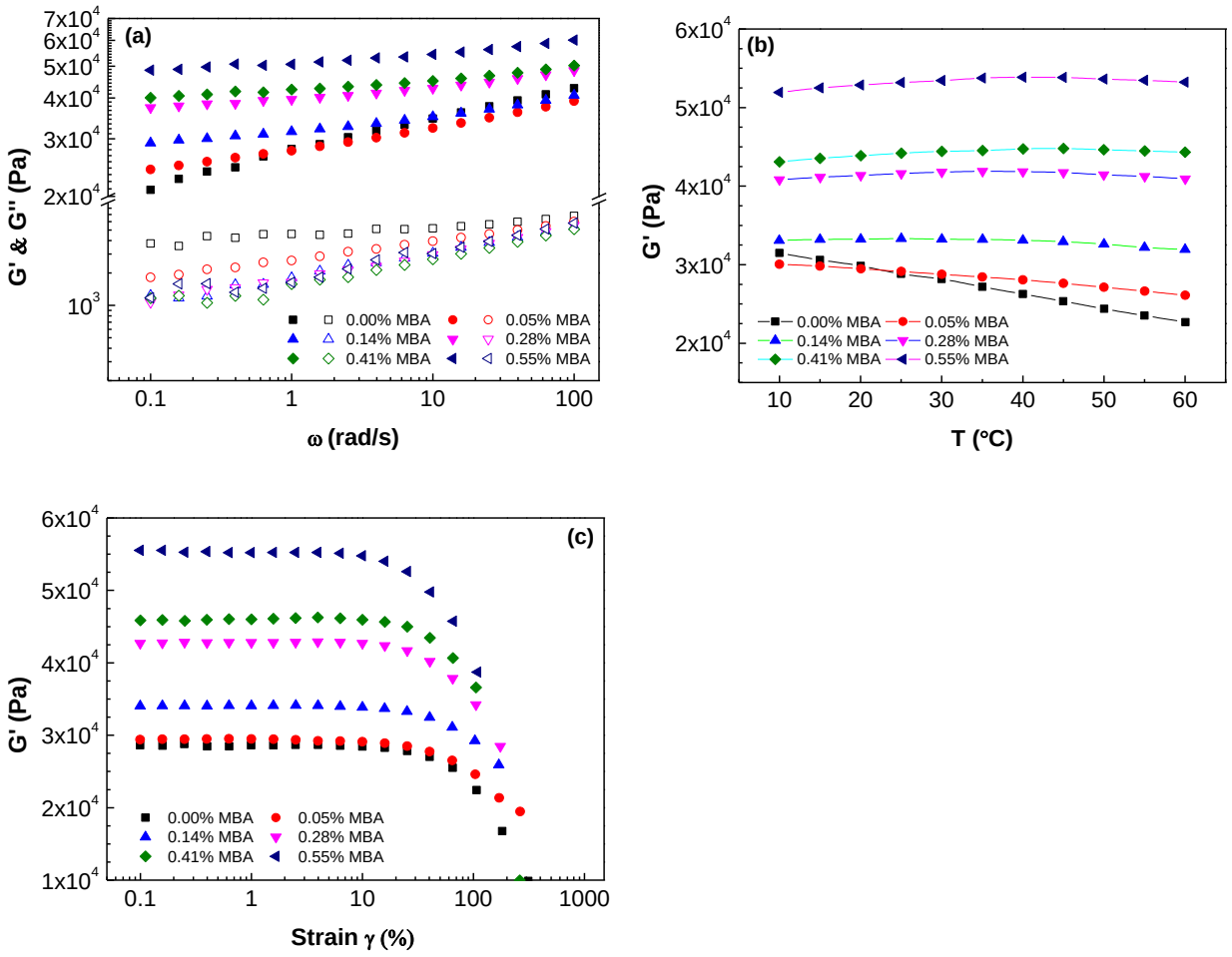

Fig. 2. (a) $G'(\omega)$ and $G''(\omega)$ as a function of frequency at $\gamma = 0.5\%$ and $T = 25$ ℃; (b) $G'(T)$ as a function of temperature at $\omega = 1$ rad/s and $\gamma = 0.5\%$; and (c) $G'(\gamma)$ as a function of strain amplitude γ at $\omega = 10$ rad/s and $T = 60$ ℃, measured for samples with different crosslinker concentrations ($\%C$).

To account for the phenomena observed above that grafted starch hydrogels with different concentrations of the crosslinker had different rheological behaviors, more discussion is presented below.

The crosslinked hydrogels showed a specific behavior when deformed at small strains, which

corresponds to a dominant and non-frequency-dependent elastic modulus (Anseth, Bowman, & Brannon-Peppas, 1996). According to the theory of rubber elasticity developed by Flory, the equilibrium shear modulus of a freshly prepared hydrogel in a non-swollen state can be expressed by the following equation: (Ferry, 1980; Kulicke & Nottelmann, 1989)

$$G_e' = \left(1 - \frac{2}{f}\right) v_e RT = \left(\frac{f-2}{2}\right) n_e RT = \frac{(f-2)C}{2M_e} RT \qquad (4)$$

where the functionality f is the number of strands linked to a crosslinker, R is the universal gas constant (8.314 J/mol/K), T is the temperature, and C is the total monomer concentration in kg/m^3. v_e, n_e and M_e respectively represent the number of elastically effective chains per unit volume, the number of elastically effective entanglement points, and the mesh width (molecular weight between two entanglement points) in the network. Equation 4 establishes a relationship between the elastic behavior of the crosslinked gel and the molecular architecture parameters of the network. A hydrogel consisting of a 3D polymer network and solvent immobilized within the network behaves as an elastic solid. As the network cannot dissipate energy through flow, the resultant G'' of the hydrogels comes from a viscous flow (η_s) of the solvent molecules within the gel, and the following equation is relevant: (Kulicke & Nottelmann, 1989)

$$G'' - \eta_s \cdot \omega \approx 0 \qquad (5)$$

The measured values of G'' are on the order of 0.1% to 5% of the value of G', therefore G'' can be neglected in calculations.

It was shown by Ball et al. (Ball, Crutchfield, & Edwards, 1960) that the decomposition of the

initiator APS neither initiated the crosslinking reaction nor the propagation of grafted side chains instantly, but induced the formation of starch ketones due to the presence of residual oxygen. This reaction had little influence on the modulus of the system, leading to a nearly constant value of G' in the induction period. After the oxygen in the system was consumed, the starch macromolecular radicals subsequently initiated the graft copolymerization of AM and the crosslinking reaction on starch macromolecules. This process led to an increase in the densities of covalent crosslinking points and non-covalent entanglement points from grafted side chains, resulting in an increase in G' as represented by Equation 4. Furthermore, a higher crosslinking density in grafted starch hydrogels corresponded to less dangling side chains including the newly formed graft side chains of PAM as well as the existing lateral starch molecular chains. These dangling chains could freely mobilize and be involved in the flow of the solvent entrapped in the network when small deformation was applied to the hydrogel. Thus, a highly crosslinked network with less dangling chains showed a smaller viscous flow (η_s) as represented in Equation 5, leading to a smaller value of G''.

The reasons why the grafted starch hydrogels prepared with different crosslinker contents showed different rheological frequency-dependencies are as follows. At low frequencies, the soft hydrogels with less crosslinking allowed the entangled dangling chains to disentangle, especially with enough time (Moura, Figueiredo, & Gil, 2007; Weng, Chen, & Chen, 2007). Therefore, the soft hydrogels showed smaller values of G' and larger values of G''. However, for the more rigid hydrogels, the covalent crosslinking bonds within the network restricted the motion of reversible physical entangled chains, thus these hydrogels presented a higher frequency-independence of G'.

The temperature-dependence of G' can be explained from the entropic and enthalpic nature of the gel elasticity. The elastic modulus G' of a gel can be written as the sum of the entropic term G_s' and the enthalpic term G_u' (Nishinari, Watase, & Ogino, 1984):

$$G' = G'_s + G'_u \qquad (6)$$

G'_s is predominant over G'_u at lower temperatures, and vice versa at higher temperatures. It may be concluded that the maximum temperature T_{max}, at which $G'_s = G'_u$ holds, was largely determined by the crosslinking density of the gel. This temperature shifted to greater values as the crosslinker concentration was increased. The grafted starch hydrogel, acting as a partial thermo-reversible gel beyond T_{max}, had $G'(T)$ decreasing with the increased temperature. This behavior could be ascribed to the fact that a significant amount of crosslinking junctions in the network were not simply covalent bonds, but secondary bonds such as hydrogen bonds or physical entanglements from the starch macromolecular chains and the grafted side chains of PAM. Thus, the entropic elasticity supported by the secondary bonds was reduced due to the disruption of these non-covalent bonds at higher temperatures, resulting in a decrease in the crosslinking density and lower values of G' of the gels, as shown in Equation 4.

3.2. Effect of initiator concentration (%I)

The microstructure of such starch graft copolymer is usually characterized by the graft frequency and the length of graft side chains, which depends largely on the number of initial radicals created on the starch backbone. This number, in turn, is usually regulated by the initiator concentration (%*I*) during the polymerization. It is thus of importance to study the relationships between the kinetics of graft copolymerization of starch, the microstructure of the gel and the initiator concentration in the reactive system. %*I* refers to the percentage quantity of initiator relative to the amount of anhydroglucose of starch.

Figure 3 shows the variations in elastic modulus $G'(t)$ (a) and viscous modulus $G''(t)$ (b) for the samples with different initiator concentrations at a constant temperature of 60 °C. For all the samples, $G'(t)$ and $G''(t)$ increased and leveled off within a certain reaction time after an induction period, except for the sample without the initiator. Therefore, significant increases in moduli were proposed to be due to the starch graft copolymerization induced by the initiator. The slightly increased $G'(t)$ of the sample with no initiator could be attributed to the slow moisture evaporation (Della Valle, Buleon, Carreau, Lavoie, & Vergnes, 1998). The induction time for the samples with different *%I* reduced with the increased content of initiator.

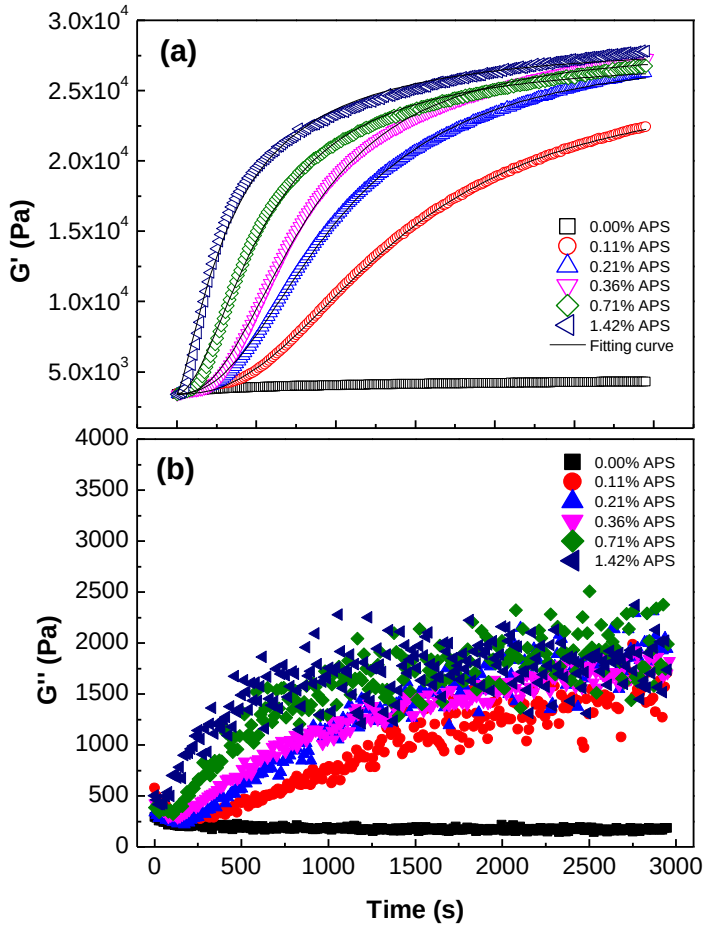

Fig. 3. Variations in (a) elastic moduli *G′* and (b) viscous moduli *G″* during graft copolymerization of NCS with 0.05% crosslinker (*%C*) and different initiator concentrations (*%I*). All measurements were performed at 60 °C under dynamic oscillations at $\omega = 1\ \mathrm{rad/s}$ and $\gamma = 0.5\%$. The solid lines in (a) represent fitting curves using Equation 1.

It could be easier to draw conclusions about the influence of the initiator concentration by studying the characteristic parameters as shown in **Table S2**. The rheokinetic parameters for these systems including the half gelation time θ, the coefficient *n*, and the gelation rate *P* had correlations with the initiator concentration with three mathematical models listed in **Table S2**. Higher *%I* led to a reduction exponentially in θ and linearly in *n* but an exponentially increase in *P*, which was consistent with the kinetics of free radical polymerization (Flory, 1953). This result indicated that the reactive mixture before loaded in the rheometer could be regarded as *completely micromixed*, under which the chemical kinetics determined the graft copolymerization process despite in a concentrated starch system. In this system given enough time for mixing, the characteristic reaction time is much larger than the characteristic time for mixing, and the improved mixing will not influence the course of the reaction significantly (Oechsler, Melo, & Pinto, 2016). Even though the initiator effect produced a great influence on the reaction kinetics, G'_∞ of all samples with an average value of 27511±2175 Pa had almost no dependence on *%I*. This suggested that *%I* had no effect on the microstructure of grafted starch hydrogels in the concentrated starch system. Moreover, the rheological behaviors from oscillatory tests in the sweeps of frequency, temperature and strain for all the samples showed the same behavior (**Fig. S2**), which further indicated that the hydrogels with different *%I* might have similar graft frequencies and lengths of graft chains.

The result that all the hydrogels with different initiator concentrations showed similar microstructures seemed to contradict the effect of the kinetics of free radical polymerization, where the lower initiator content should yield fewer PAM grafts with a higher molecular weight for the grafted starch. Willett and Finkenstadt (2003) reported that grafted starch hydrogels had similar graft frequency and length of graft side chains in REX, regardless of the initiator content. It was also found that the initial efficiency of APS was as low as a few percent, likely due to its strong effect of the induced decomposition and the cage effect in REX with a high viscosity. The similar structures of the grafted starch hydrogels with different initiator concentrations might be ascribed to the strong possibility of the chain transfer reactions between starch macromolecules and propagating chain radicals in the concentrated starch system (Willett & Finkenstadt, 2009). The graft copolymerization could also be initiated by the chain transfer reaction, which would facilitate the generation of the starch macromolecular initial radicals, rather than is a simple initiator-based grafting process.

3.3. Effect of reaction temperature (T_r)

The temperature of graft copolymerization can influence the reactivity of monomer molecules (the Arrhenius law) as well as the rheological behaviors of the concentrated starch system (the Trommsdorff effect), therefore causing various effects on the reaction kinetics, such as the rate of dissociation of the initiator (APS), the propagation and termination of graft side chains, and the tendency for the chain transfer reaction to occur. (Flory, 1953)

Figure 4 illustrates the moduli $G'(t)$ and $G''(t)$ recorded during the NCS starch graft copolymerization with *%C* of 0.05% and *%I* of 0.36% for different T_r, ranging from 50 to 80 ℃. $G'(t)$ and $G''(t)$ behaved similarly among different samples, except for the sample synthesized in $T_r = 50$ ℃, of which a steady state modulus had not been reached before the cessation of monitoring time, due to its

slow polymerization rate at this low temperature. Furthermore, the induction time decreased with an increase in T_r, and the effect of T_r on the induction time was similar to that of the initiator concentration as discussed above.

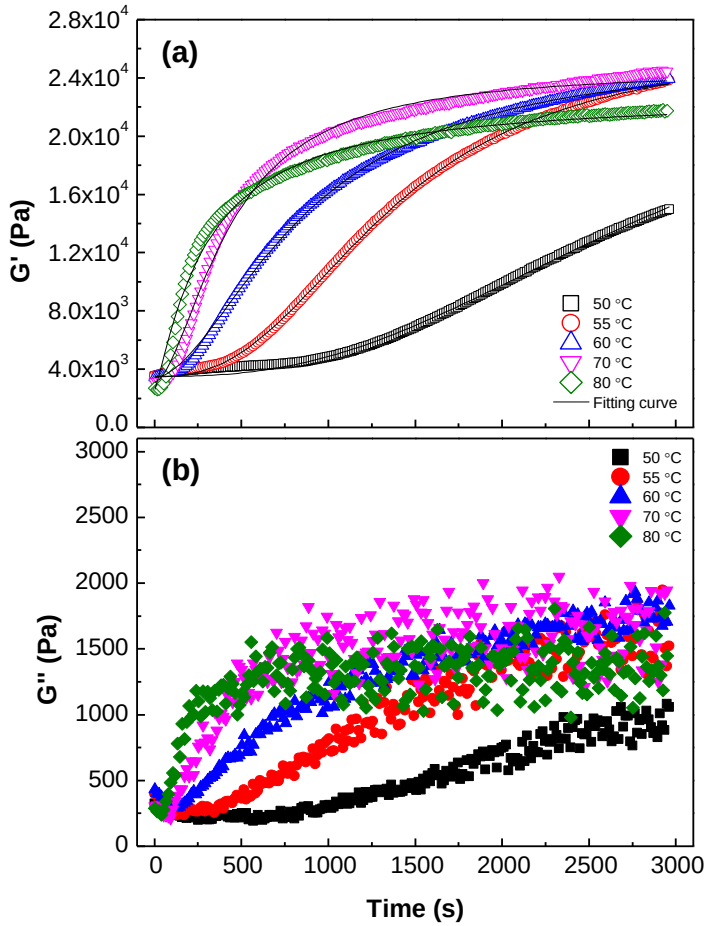

Fig. 4. Variations in (a) elastic moduli *G'* and (b) viscous moduli *G''* during graft copolymerization of NCS with 0.05% crosslinker (*%C*) and 0.36% initiator (*%I*) at different reaction temperatures (T_r). All measurements were performed under dynamic oscillations at $\omega = 1$ rad/s and $\gamma = 0.5\%$. The solid lines in (a) represent fitting curves using Equation 1.

394

395 The effect of T_r can be well compared using the extracted data of G'_∞, θ, *n* and *P* in **Table S3** as
396 before. The half gelation time θ decreased exponentially with an increase in T_r, accompanying by a
397 randomly decreasing behavior of the coefficient *n*. This rheokinetic behavior was consistent with the
398 free radical polymerization kinetics (Flory, 1953). Similar to the effect of the initiator content, the results
399 from reaction temperature effect also indicated that the reactive mixture of the starch melt acquired from
400 the mixing processing was completely micromixed. The gelation rate *P* attained a maximum value of
401 22.59 Pa/s at $T_r = 70$ ℃. There was some difference between the steady state values of G'_∞ measured
402 at T_r and those measured after the polymerization at $T = 25$ ℃, regarding the
403 temperature-dependence of moduli represented in Equation 4. When T_r was varied from 55 to 80 °C, it
404 had little effect on G'_∞ ($T = 25$ ℃), which had a mean value of 29482±346 Pa. This was in an
405 agreement with the results regarding the graft parameters for the grafted starch prepared by REX as
406 reported by Willett and Finkenstadt (2003). The dynamic oscillatory tests in frequency, temperature and
407 strain displayed a similar behavior for the samples synthesized with different T_r (see **Fig. S3**), except
408 for the sample prepared at $T_r = 50$ ℃, of which the reaction had not been complete. It can be
409 concluded that T_r had little influence on the microstructure of the final grafted starch hydrogels in the
410 concentrated starch system.

411 Interestingly, T_r had little effect on the rheological properties of the final grafted starch gel in the
412 concentrated starch system, despite its great influence on the hydrogel microstructure in a dilute system.
413 This fact has been confirmed by the findings from Willett and Finkenstadt (2003), where the grafted
414 starches prepared from the same formulation with different T_r showed almost similar graft parameters
415 including the monomer conversion, grafting efficiency, and graft frequency. A higher value of T_r
416 corresponded to higher polymerization rate constants relating to the initiation, propagation, termination,

and chain transfer according to the Arrhenius law, which gave the starch grafts a wider polydispersity with shorter graft chain lengths. Conversely, a lower viscosity of the system at higher T_r corresponded to a greater mobility of the monomer and a reduced Trommsdorff effect, which was beneficial to the graft polymerization in the concentrated starch system. These two counteracting effects controlled by the temperature led to the result that the grafted starch hydrogels prepared from different T_r possessed similar microstructures.

3.4. Effect of amylose/amylopectin ratio

During the starch graft copolymerization, the rheological behaviors in a REX system could remarkably influence the mobility of the monomer due to the Trommsdorff effect (Flory, 1953). Xie et al. (2009) reported that various corn starches with different amylose/amylopectin ratios also showed different rheological properties. In this work, four types of corn starch with different amylose/amylopectin ratios were chosen to study their reaction rheokinetics and microstructure of final grafted starch hydrogels.

Figure 5 showed that for the four types of grafted starch hydrogel with different amylose/amylopectin ratios, $G'(t)$ and $G''(t)$ exhibited the same trend with time as described above. The rheokinetic parameters obtained from fitting curves were illustrated in **Table S4**. The higher the ratios of amylose to amylopectin in starch, the higher the values of steady-state modulus G'_∞ and the gelation rate P. However, the half gelation time θ and the coefficient n were nearly independent of the starch type with apparent values of 850±143 s and 2.12±0.06 respectively. This finding indicated that the rheological behaviors of starch melt had little influence on the extent of micromixing for four types of starch given enough mixing time.

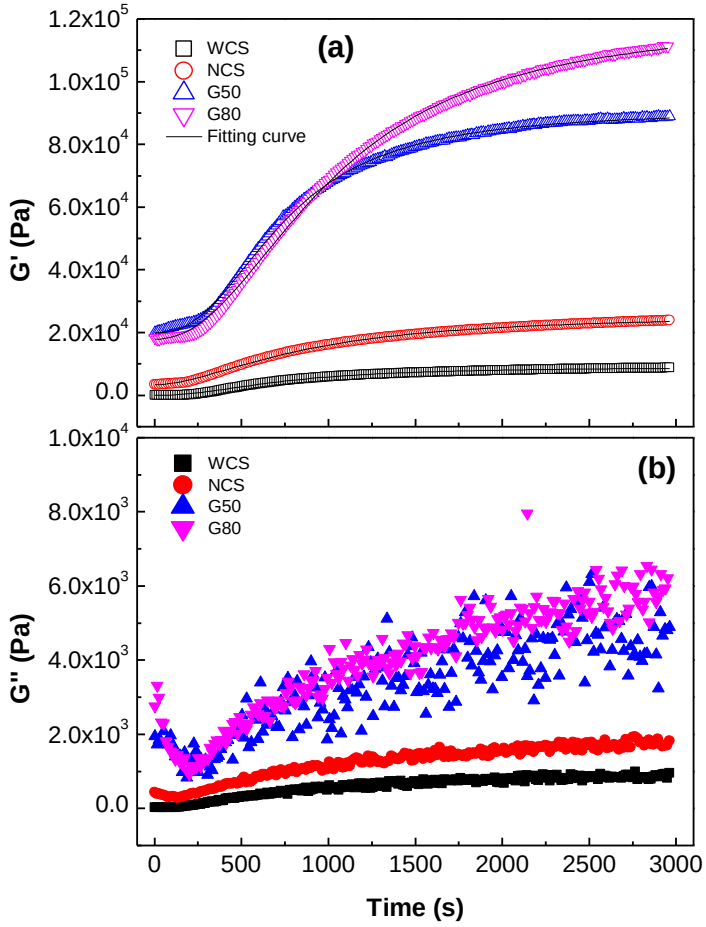

Fig. 5. Variations in (a) elastic moduli G' and (b) viscous moduli G'' during graft copolymerization for WCS, NCS, G50 and G80 with 0.05% crosslinker ($\%C$) and 0.36% initiator ($\%I$) at $T_r = 60$℃. All measurements were performed under dynamic oscillations at $\omega = 1$ rad/s and $\gamma = 0.5\%$. The solid lines in (a) represent fitting curves using Equation 1.

The results of oscillatory frequency tests (see **Fig. 6a**) revealed that the grafted starch hydrogels with higher amylose contents (G50 and G80) had less dependence on frequency for G' (smaller n'), and greater for G'' (larger n''), as represented in Equation 3. **Fig. 6b** showed the temperature-dependence

behaviors of *G'* for the four types of grafted starch hydrogel. It was found that for the hydrogels prepared from WCS and NCS, *G'* showed a slight decrease with the increased temperature. In contrast, for the samples originated from G50 and G80, *G'* increased slightly from 10 to 15 °C, and then decreased significantly to about three quarters of the maximum value of *G'* at 80 °C. This behavior was presumably attributed to the presence of large amounts of hydrogen bonds in the high-amylose starch gels which were sensitive to the temperature variation (Xie, Halley, & Avérous, 2012). The oscillatory strain test results in **Fig. 6c** showed that the hydrogel prepared from WCS had the widest linear viscoelastic region ($\gamma = 40.1\%$), followed by NCS ($\gamma = 10.0\%$), G50 ($\gamma = 1.0\%$), and G80 ($\gamma = 0.6\%$). This also indicated that $\gamma = 0.5\%$ was suitable for all the four types of hydrogel.

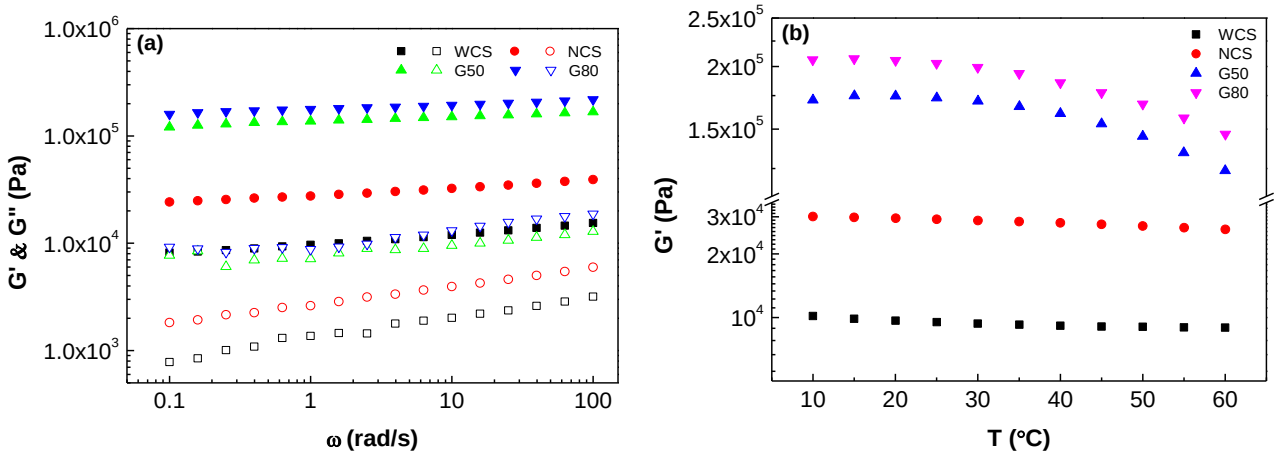

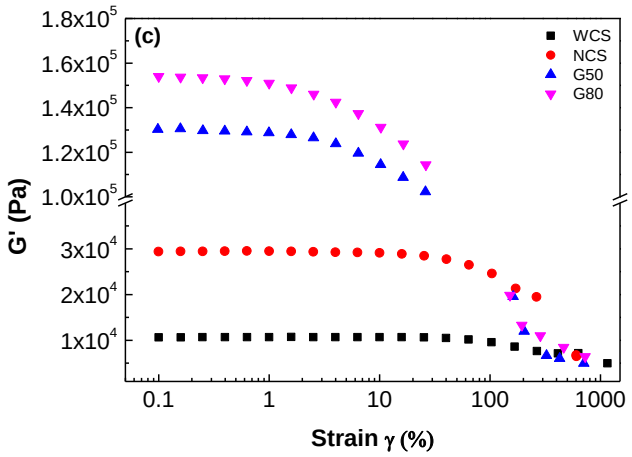

Fig. 6. (a) $G'(\omega)$ and $G''(\omega)$ as a function of frequency at $\gamma = 0.5\%$ and $T = 25$ ℃; (b) $G'(T)$ as a function of temperature at $\omega = 1$ rad/s and $\gamma = 0.5\%$; and (c) $G'(\gamma)$ as a function of strain amplitude γ at $\omega = 10$ rad/s and $T = 60$ ℃, measured for samples obtained from starches with different amylose/amylopectin ratios.

The grafted starch hydrogels prepared from the four starches with different amylose/amylopectin ratios showed diverse reaction rheokinetics and rheological behaviors. These behaviors could be ascribed to the properties of amylose and amylopectin in the starch. When the starch suspension was heated under shear stress, a separation of amylose and amylopectin presented in the starch granule would occur, due to these two types of macromolecules being thermodynamically incompatible. The starch melt gradually formed a physical entanglement network in the concentrated starch system. In this network, the largely unbranched amylose component tended to form intermolecular hydrogen bonds and acted as a matrix, with the highly branched amylopectin performing as a filler between the amylose matrix (Ai & Jane, 2015; Keetels, Van Vliet, & Walstra, 1996). More amylose in high-amylose starches (G50 and G80) would be involved in the construction of a 3D matrix, resulting in a higher crosslinking density of the hydrogels originated from G50 and G80 with higher values of G'_{∞} according to Equation

4. Thus, the G50- and G80-based hydrogels had a narrower linear viscoelastic region and their G' values showed lower frequency-dependence but higher temperature-dependence. All of these rheological behaviors indicated a large amount of physical crosslinking junctions contained in the hydrogels prepared from high-amylose starches (G50 and G80), compared with low-amylose starches (WCS and NCS). It would be worth to undertake further research to understand the relationship between rheological behaviors of starch melt and the graft copolymerization efficiency and thus the effects of amylose/amylopectin ratio on the microstructure of starch-based hydrogels. It is noteworthy that although the inevitable formation of homopolymer in the experiments could contribute to the rheological results, this effect could be minimal and thus was not separately considered for the rheokinetic modeling here. Nevertheless, it is worth for future research to study any possible effect of the homopolymer on the rheological properties of the starch graft copolymer.

4. Conclusions

By the *in-situ* synthesis of starch-*g*-PAM in a rheometer, we established a new method to probe the rheokinetics of graft copolymerization in concentrated starch through dynamic shear oscillation measurements. We found that the reaction rheokinetic behaviors of starch melt could be well represented by a modified Hill equation. The rheokinetics of starch graft copolymerization was consistent with the chemical reaction kinetics, indicating that the starch melt mixtures were completely micromixed and that the graft copolymerization of concentrated starch was predominated by the reaction kinetics rather than by the diffusion rate of mass transfer.

With an increased amount of the crosslinker, there was a linear increase in G', accompanied by a decreased mesh size and enhanced thermal stability of the starch hydrogel. Interestingly, the initiator content and the reaction temperature had little influence on the final microstructure of the hydrogel,

504 despite their significant impact on the reaction kinetics. This unusual phenomenon could be most likely
505 due to the strong effect from the induced decomposition of the initiator and the chain transfer reaction in
506 the concentrated starch system. Moreover, the hydrogels originating from amylose-rich starches (G50
507 and G80) had a higher crosslinking density, but a lower thermal stability of the 3D network, due to the
508 formation of large amounts of hydrogen bonds by amylose.

509 The knowledge obtained from this work could guide the rational design of REX processes to
510 produce grafted polysaccharide hydrogels with desired structure and properties, as shown in the
511 following points:

512 1) To improve the starch grafting efficiency during REX, enhancing the distributive and
513 dispersive mixing of reactants before chemical reaction in an extruder, instead of during the
514 reaction, can be an effective strategy.

515 2) The microstructure of starch-based hydrogels produced by REX can be effectively regulated
516 with the crosslinker.

517 3) The mathematic models of rheokinetics deduced depending on the temperature and initiator
518 effects can be used to control the reaction time on behalf of the limited residence time
519 during REX.

520

521

522 **Acknowledgements**

523 This work has been financially supported by the NSFC (Project No. 31571789) and the 111 Project
524 (B17018). X. Bao would like to thank the Oversea Study Program of Guangzhou Elite Project (GEP) for
525 providing research funding for his studies at Monash University and the Commonwealth Science and

Industrial Research Organisation (CSIRO), Australia. F. Xie acknowledges the European Union's Marie Skłodowska-Curie Actions (MSCA) and the Institute of Advanced Study (IAS), University of Warwick for the Warwick Interdisciplinary Research Leadership Programme (WIRL-COFUND). L. Zhong would like to thank the support of the Research Funds for Universities in Guangxi (No. KY2015ZD040).

References

Ahmed, E. M. (2015). Hydrogel: Preparation, characterization, and applications: A review. *Journal of Advanced Research, 6*(2), 105-121.

Ai, Y., & Jane, J. l. (2015). Gelatinization and rheological properties of starch. *Starch - Stärke, 67*(3-4), 213-224.

Anseth, K. S., Bowman, C. N., & Brannon-Peppas, L. (1996). Mechanical properties of hydrogels and their experimental determination. *Biomaterials, 17*(17), 1647-1657.

Ball, D., Crutchfield, M. M., & Edwards, J. O. (1960). The mechanism of the oxidation of 2-propanol by peroxydisulfate ion. *the Journal of Organic Chemistry, 25*(9), 1599-1611.

Bao, X., Ali, A., Qiao, D., Liu, H., Chen, L., & Yu, L. (2015). Application of polymer materials in developing slow/control release fertilizer. *Acta Polymerica Sinica*(9), 1010-1019.

Calvet, D., Wong, J. Y., & Giasson, S. (2004). Rheological monitoring of polyacrylamide gelation: Importance of cross-link density and temperature. *Macromolecules, 37*(20), 7762-7771.

Carr, M., Kim, S., Yoon, K., & Stanley, K. (1992). Graft polymerization of cationic methacrylate, acrylamide, and acrylonitrile monomers onto starch by reactive extrusion. *Cereal Chemistry, 69*(1), 70-75.

Cayuela, J., Da Cruz-Boisson, F., Michel, A., Cassagnau, P., & Bounor-Legaré, V. (2016). Synthesis of bisphenol-A polycarbonate-poly (ε-caprolactone) copolymers by reactive extrusion through in situ ε-caprolactone polymerization. *Polymer, 104*, 156-169.

Cicuta, P., & Donald, A. M. (2007). Microrheology: a review of the method and applications. *Soft Matter, 3*(12), 1449-1455.

Dai, L., Wang, B., An, X., Zhang, L., Khan, A., & Ni, Y. (2017). Oil/water interfaces of guar gum-based biopolymer hydrogels and application to their separation. *Carbohydrate Polymers, 169*, 9-15.

Della Valle, G., Buleon, A., Carreau, P., Lavoie, P.-A., & Vergnes, B. (1998). Relationship between structure and viscoelastic

behavior of plasticized starch. *Journal of Rheology, 42*(3), 507-525.

El-Saied, H., Waly, A. I., & Basta, A. H. (2000). High water absorbents from lignocelluloses. I. Effect of reaction variables on the water absorbency of polymerized lignocelluloses. *Polymer-Plastics Technology and Engineering, 39*(5), 905-926.

El-Saied, H., Waley, A. I., Basta, A. H., & El-Hadi, O. (2004). High water absorbents from lignocelluloses. II. Novel soil conditioners for sandy soil from lignocellulosic wastes. *Polymer-Plastics Technology and Engineering, 43*(3), 779-795.

El-Saied, H., Basta, A. H., El-Hadi, O., & Waley, A. I. (2007). High water absorbents from lignocelluloses. Part III: Upgrading the utilization of old newspaper [ONP] in agronomic application. *Polymer-Plastics Technology and Engineering, 46*(3), 311-319.

Elbarbary, A. M., El-Rehim, H. A. A., El-Sawy, N. M., Hegazy, E.-S. A., & Soliman, E.-S. A. (2017). Radiation induced crosslinking of polyacrylamide incorporated low molecular weights natural polymers for possible use in the agricultural applications. *Carbohydrate Polymers, 176*, 19-28.

Ferry, J. D. (1980). *Viscoelastic Properties of Polymers*. (third ed.). Canada: John Wiley & Sons.

Finkenstadt, V. L., & Willett, J. L. (2005). Reactive extrusion of starch‐polyacrylamide graft copolymers: effects of monomer/starch ratio and moisture content. *Macromolecular Chemistry and Physics, 206*(16), 1648-1652.

Flory, P. J. (1953). *Principles of Polymer Chemistry*. (First ed.). Ithaca: Cornell University Press.

Formela, K., Hejna, A., Haponiuk, J., & Tercjak, A. (2017). In situ processing of biocomposites via reactive extrusion. In D. Ray (Ed.), *Biocomposites for High-Performance Applications: Current Barriers and Future Needs Towards Industrial Development* (pp. 195-246). Woodhead Publishing.

Garcia-Garcia, D., Rayón, E., Carbonell-Verdu, A., Lopez-Martinez, J., & Balart, R. (2017). Improvement of the compatibility between poly (3-hydroxybutyrate) and poly (ε-caprolactone) by reactive extrusion with dicumyl peroxide. *European Polymer Journal, 86*, 41-57.

Giraldo, J., Vivas, N. M., Vila, E., & Badia, A. (2002). Assessing the (a) symmetry of concentration-effect curves: empirical versus mechanistic models. *Pharmacology & Therapeutics, 95*(1), 21-45.

Guilherme, M. R., Aouada, F. A., Fajardo, A. R., Martins, A. F., Paulino, A. T., Davi, M. F., et al. (2015). Superabsorbent hydrogels based on polysaccharides for application in agriculture as soil conditioner and nutrient carrier: A review. *European Polymer Journal, 72*, 365-385.

Ibrahim, M. M., Abd‐Eladl, M., & Abou‐Baker, N. H. (2015). Lignocellulosic biomass for the preparation of cellulose‐based hydrogel and its use for optimizing water resources in agriculture. *Journal of Applied Polymer Science, 132*(42).

Ismail, H., Irani, M., & Ahmad, Z. (2013). Starch-based hydrogels: present status and applications. *International Journal of Polymeric Materials and Polymeric Biomaterials, 62*(7), 411-420.

Janssen, L. P. (2004). *Reactive Extrusion Systems*. New York: CRC Press.

Kashyap, P. L., Xiang, X., & Heiden, P. (2015). Chitosan nanoparticle based delivery systems for sustainable agriculture. *International Journal of Biological Macromolecules, 77*, 36-51.

Keetels, C., Van Vliet, T., & Walstra, P. (1996). Gelation and retrogradation of concentrated starch systems: 1 Gelation. *Food Hydrocolloids, 10*(3), 343-353.

Khalid, I., Ahmad, M., Minhas, M. U., & Barkat, K. (2017). Synthesis and evaluation of chondroitin sulfate based hydrogels of loxoprofen with adjustable properties as controlled release carriers. *Carbohydrate Polymers*.

Kulicke, W. M., & Nottelmann, H. (1989). Structure and swelling of some synthetic, semisynthetic, and biopolymer hydrogels. In J. E. Glass (Ed.), *Polymers in Aqueous Media* (pp. 15-44). ACS Publications.

Lam, J., Clark, E. C., Fong, E. L., Lee, E. J., Lu, S., Tabata, Y., et al. (2016). Evaluation of cell-laden polyelectrolyte hydrogels incorporating poly (l-Lysine) for applications in cartilage tissue engineering. *Biomaterials, 83*, 332-346.

Luo, S., Cao, J., & McDonald, A. G. (2016). Interfacial improvements in a green biopolymer alloy of poly (3-hydroxybutyrate-co-3-hydroxyvalerate) and lignin via in situ reactive extrusion. *ACS Sustainable Chemistry & Engineering, 4*(6), 3465-3476.

Madbouly, S. A., & Otaigbe, J. U. (2005). Rheokinetics of thermal-induced gelation of waterborne polyurethane dispersions. *Macromolecules, 38*(24), 10178-10184.

Moad, G. (2011). Chemical modification of starch by reactive extrusion. *Progress in Polymer Science, 36*(2), 218-237.

Mohammadi, Z., Sun, S., Berkland, C., & Liang, J. T. (2017). Chelator-mimetic multi-functionalized hydrogel: Highly efficient and reusable sorbent for Cd, Pb, and As removal from waste water. *Chemical Engineering Journal, 307*, 496-502.

Moura, M. J., Figueiredo, M. M., & Gil, M. H. (2007). Rheological study of genipin cross-linked chitosan hydrogels. *Biomacromolecules, 8*(12), 3823-3829.

Nishinari, K., Watase, M., & Ogino, K. (1984). On the temperature dependence of the elasticity of agarose gels.

Macromolecular Chemistry and Physics, 185(12), 2663-2668.

Oechsler, B. F., Melo, P. A., & Pinto, J. C. (2016). Micromixing effects on the dynamic behavior of continuous stirred tank reactors. *Applied Mathematical Modelling, 40*(7), 4778-4794.

Ojijo, V., & Ray, S. S. (2015). Super toughened biodegradable polylactide blends with non-linear copolymer interfacial architecture obtained via facile in-situ reactive compatibilization. *Polymer, 80*, 1-17.

Perez, J. J., & Francois, N. J. (2016). Chitosan-starch beads prepared by ionotropic gelation as potential matrices for controlled release of fertilizers. *Carbohydrate Polymers, 148*, 134-142.

Qiao, D., Liu, H., Yu, L., Bao, X., Simon, G. P., Petinakis, E., et al. (2016). Preparation and characterization of slow-release fertilizer encapsulated by starch-based superabsorbent polymer. *Carbohydrate Polymers, 147*, 146-154.

Sarkar, D. J., & Singh, A. (2017). Base triggered release of insecticide from bentonite reinforced citric acid crosslinked carboxymethyl cellulose hydrogel composites. *Carbohydrate Polymers, 156*, 303-311.

Singh, B., Sharma, D., Negi, S., & Dhiman, A. (2015). Synthesis and characterization of agar-starch based hydrogels for slow herbicide delivery applications. *International Journal of Plastics Technology, 19*(2), 263-274.

Sun, Y., Ma, Y., Fang, G., Ren, S., & Fu, Y. (2016). Controlled pesticide release from porous composite hydrogels based on lignin and polyacrylic acid. *Bioresources, 11*(1), 2361-2371.

Takenaka, M., Kobayashi, T., Hashimoto, T., & Takahashi, M. (2002). Time evolution of dynamic shear moduli in a physical gelation process of 1, 3: 2, 4-bis-O-(p-methylbenzylidene)-D-sorbitol in polystyrene melt: Critical exponent and gel strength. *Physical Review E, 65*(4), 041401.

Ullah, F., Othman, M. B. H., Javed, F., Ahmad, Z., & Akil, H. M. (2015). Classification, processing and application of hydrogels: A review. *Materials Science and Engineering: C, 57*, 414-433.

Waigh, T. A. (2016). Advances in the microrheology of complex fluids. *Reports on Progress in Physics, 79*(7), 074601.

Wei, L., McDonald, A. G., & Stark, N. M. (2015). Grafting of bacterial polyhydroxybutyrate (PHB) onto cellulose via in situ reactive extrusion with dicumyl peroxide. *Biomacromolecules, 16*(3), 1040-1049.

Weng, L., Chen, X., & Chen, W. (2007). Rheological characterization of in situ crosslinkable hydrogels formulated from oxidized dextran and N-carboxyethyl chitosan. *Biomacromolecules, 8*(4), 1109-1115.

Willett, J. L., & Finkenstadt, V. L. (2003). Preparation of strach‐graft‐polyacrylamide copolymers by reactive extrusion. *Polymer Engineering & Science, 43*(10), 1666-1674.

Willett, J. L., & Finkenstadt, V. L. (2006a). Initiator effects in reactive extrusion of starch–polyacrylamide graft copolymers.

637 *Journal of Applied Polymer Science, 99*(1), 52-58.
638 Willett, J. L., & Finkenstadt, V. L. (2006b). Reactive extrusion of starch–polyacrylamide graft copolymers using various
639 starches. *Journal of Polymers and the Environment, 14*(2), 125-129.
640 Willett, J. L., & Finkenstadt, V. L. (2009). Comparison of Cationic and Unmodified Starches in Reactive Extrusion of Starch–
641 Polyacrylamide Graft Copolymers. *Journal of Polymers and the Environment, 17*(4), 248-253.
642 Willett, J. L., & Finkenstadt, V. L. (2015). Starch‐poly (acrylamide‐co‐2‐acrylamido‐2‐methylpropanesulfonic acid)
643 graft copolymers prepared by reactive extrusion. *Journal of Applied Polymer Science, 132*(33).
644 Winter, H. H., & Chambon, F. (1986). Analysis of linear viscoelasticity of a crosslinking polymer at the gel point. *Journal of*
645 *Rheology, 30*(2), 367-382.
646 Witono, J., Noordergraaf, I., Heeres, H., & Janssen, L. (2017). Rheological behavior of reaction mixtures during the graft
647 copolymerization of cassava starch with acrylic acid. *Polymer Engineering & Science*.
648 Xiao, X., Yu, L., Xie, F., Bao, X., Liu, H., Ji, Z., et al. (2017). One-step method to prepare starch-based superabsorbent
649 polymer for slow release of fertilizer. *Chemical Engineering Journal, 309*, 607-616.
650 Xie, F., Yu, L., Liu, H., & Chen, L. (2006). Starch modification using reactive extrusion. *Starch-Starke, 58*(3-4), 131-139.
651 Xie, F., Yu, L., Su, B., Liu, P., Wang, J., Liu, H., et al. (2009). Rheological properties of starches with different
652 amylose/amylopectin ratios. *Journal of Cereal Science, 49*(3), 371-377.
653 Xie, F., Halley, P. J., & Avérous, L. (2012). Rheology to understand and optimize processibility, structures and properties of
654 starch polymeric materials. *Progress in Polymer Science, 37*(4), 595-623.
655 Xu, P., Zeng, Q., Cao, Y., Ma, P., Dong, W., & Chen, M. (2017). Interfacial modification on polyhydroxyalkanoates/starch
656 blend by grafting in-situ. *Carbohydrate Polymers, 174*, 716-722.
657 Yang, X., Clénet, J., Xu, H., Odelius, K., & Hakkarainen, M. (2015). Two step extrusion process: from thermal recycling of
658 PHB to plasticized PLA by reactive extrusion grafting of PHB degradation products onto PLA chains.
659 *Macromolecules, 48*(8), 2509-2518.
660 Yoon, K., Carr, M., & Bagley, E. (1992). Reactive extrusion vs. batch preparation of starch–g–polyacrylonitrile. *Journal of*
661 *Applied Polymer Science, 45*(6), 1093-1100.
662 Zhang, H., Luan, Q., Huang, Q., Tang, H., Huang, F., Li, W., et al. (2017a). A facile and efficient strategy for the fabrication
663 of porous linseed gum/cellulose superabsorbent hydrogels for water conservation. *Carbohydrate Polymers, 157*,
664 1830-1836.

665 Zhang, H., Yang, M., Luan, Q., Tang, H., Huang, F., Xiang, X., et al. (2017b). Cellulose Anionic Hydrogels Based on
666 Cellulose Nanofibers As Natural Stimulants for Seed Germination and Seedling Growth. *Journal of Agricultural and*
667 *Food Chemistry, 65*(19), 3785-3791.
668 Zhang, Y., Li, H., Li, X., Gibril, M. E., & Yu, M. (2014). Chemical modification of cellulose by in situ reactive extrusion in
669 ionic liquid. *Carbohydrate Polymers, 99*, 126-131.
670 Zhang, Y., & Xu, S. (2017). Effects of amylose/amylopectin starch on starch‐based superabsorbent polymers prepared by
671 γ‐radiation. *Starch‐Stärke, 69*(1-2).
672 Zhou, J., Yu, W., & Zhou, C. (2009). Rheokinetic study on homogeneous polymer reactions in melt state under strong flow
673 field. *Polymer, 50*(18), 4397-4405.
674

– Supplementary Data –

Rheokinetics of graft copolymerization of acrylamide in concentrated starch and rheological behaviors and microstructures of reaction products

Xianyang Bao[a,b,c], Long Yu[a,d,*], George P. Simon[b], Shirley Shen[c], Fengwei Xie[e,f,g,†], Hongsheng Liu[a,d], Ling Chen[a], Lei Zhong[h]

[a] *Center for Polymer from Renewable Resources, SFSE, South China University of Technology, Guangzhou, Guangdong 510640, China*

[b] *Department of Materials Science and Engineering, Monash University, Melbourne, Vic 3800, Australia*

[c] *CSIRO Manufacturing, Bayview Avenue, Clayton, Vic 3168, Australia*

[d] *Sino-Singapore International Joint Research Institute, Guangzhou, Guangdong 510663, China*

[e] *Institute of Advanced Study, University of Warwick, Coventry CV4 7HS, United Kingdom*

[f] *International Institute for Nanocomposites Manufacturing (IINM), WMG, University of Warwick, Coventry CV4 7AL, United Kingdom*

[g] *School of Chemical Engineering, The University of Queensland, Brisbane, Qld 4072, Australia*

[h] *School of Chemistry and Chemical Engineering, Guangxi Key Laboratory Cultivation Base for Polysaccharide Materials and Modifications, Guangxi University for Nationalities, Nanning, Guangxi, China*

---

[*] Corresponding author. Email: felyu@scut.edu.cn (L. Yu)

[†] Corresponding author. Email: f.xie@uq.edu.au, fwhsieh@gmail.com (F. Xie)

1 FTIR analysis

FTIR spectra were acquired using a Nicolet 6700 FTIR spectrometer (Waltham, MA, USA) equipped with a Smart ITR. Spectra were collected at a resolution of 4 cm^{-1} in the range of 4000–600 cm^{-1} for a total of 64 scans. All the spectra were baseline corrected and normalized using OMNIC software before further analysis. Before FTIR characterization, starch-based hydrogels synthesized *in situ* was immersed in 30/70 ethanol/water (v/v) for 24 h at room temperature to extract the soluble fraction including unreacted monomer and homo-polyacrylamide. The purified starch-based hydrogels were collected by filtration and dried.

The FTIR spectra of native starch and starch-based hydrogels are shown in the **Fig. S1**. Native starch exhibited a characteristic IR absorption peak, including O-H stretching (ν_1 = 3287 cm^{-1}), C-H stretching (ν_2 = 2930 cm^{-1}), and C-O-C stretching (a triplet peak ν_3 = 1149, 1077, and 996 cm^{-1}) (Qiao et al., 2016; Zhang et al., 2014). Starch-based hydrogels not only showed a typical absorption pattern of native starch but also that of polyacrylamide (PAM). The bands at ν_4 = 1659, ν_5 = 1609, and ν_6 = 1411 were attributed to the C=O stretching, N-H bending, and C-N stretching of the amide bands in the grafted chains (PAM), respectively (Qiao, Yu, Bao, Zhang, & Jiang, 2017; Zou et al., 2012). All of these results indicated the occurrence of graft copolymerization of acrylamide onto starch in the concentrated starch system.

2 Figures

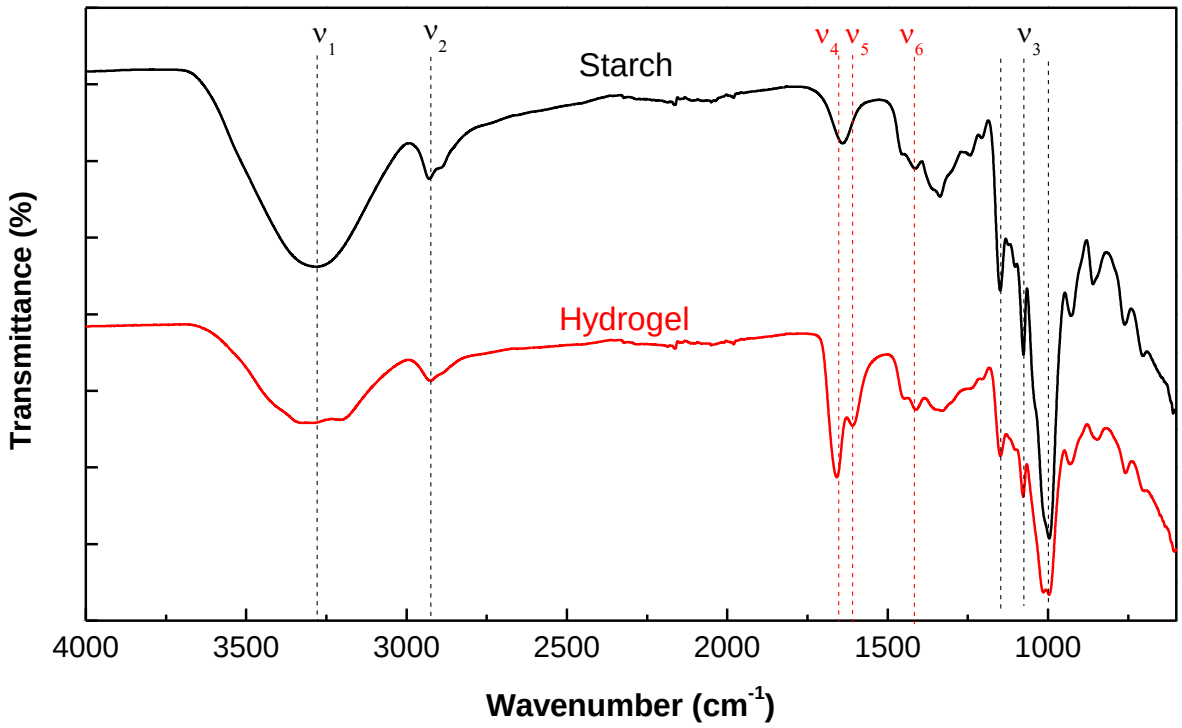

Fig. S1. FTIR spectra of starch and starch-based hydrogel. NCS was used with $T_r = 60$ ℃, $\%C = 0.05\%$, and $\%I = 0.36\%$.

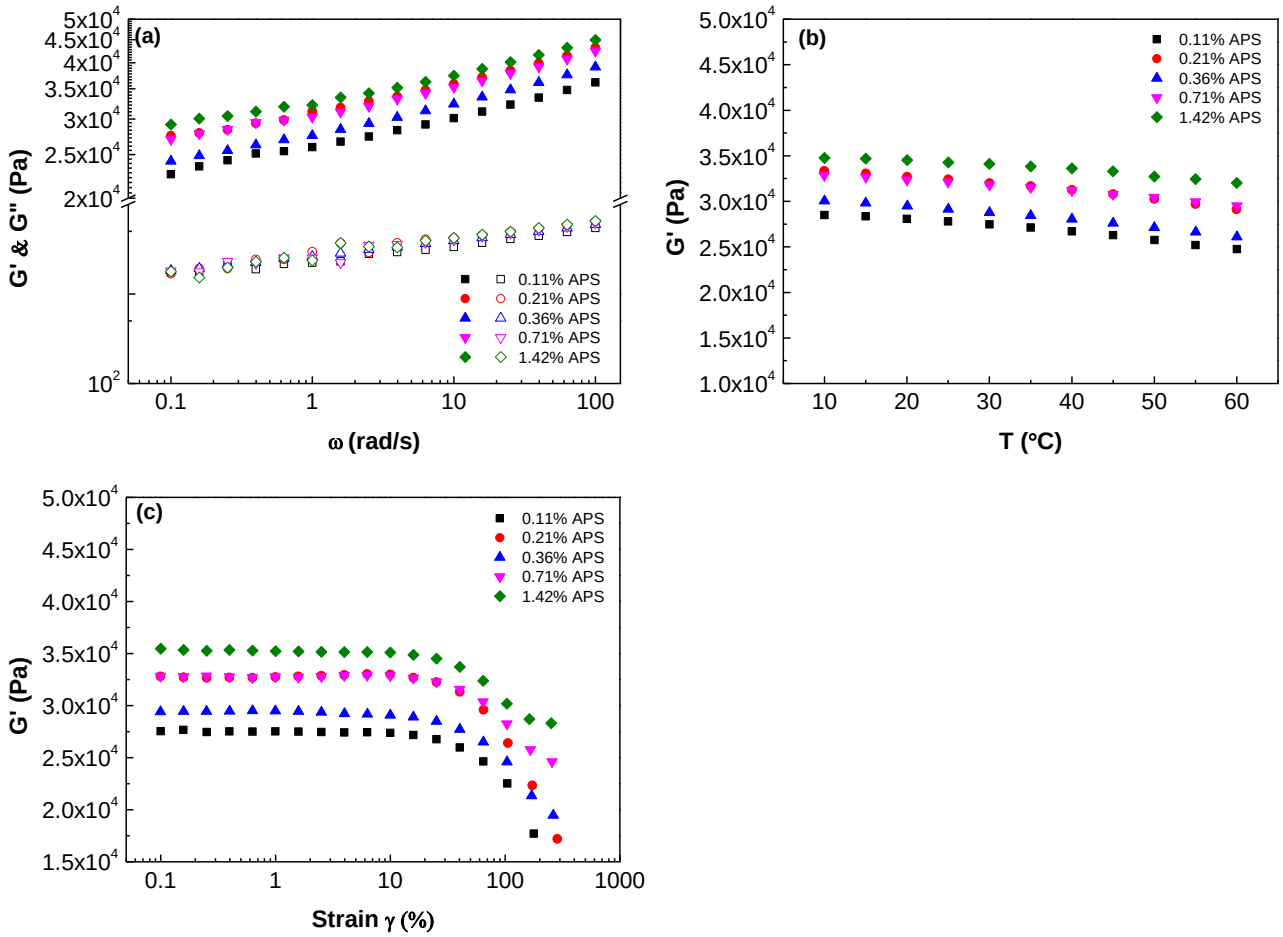

Fig. S2. (a) $G'(\omega)$ and $G''(\omega)$ as a function of frequency at $\gamma = 0.5\%$ and $T = 25$ ℃; (b) $G'(T)$ as a function of temperature at $\omega = 1$ rad/s and $\gamma = 0.5\%$; and (c) $G'(\gamma)$ as a function of strain amplitude γ at $\omega = 10$ rad/s and $T = 60$ ℃, measured for samples with different initiator concentrations ($\%I$).

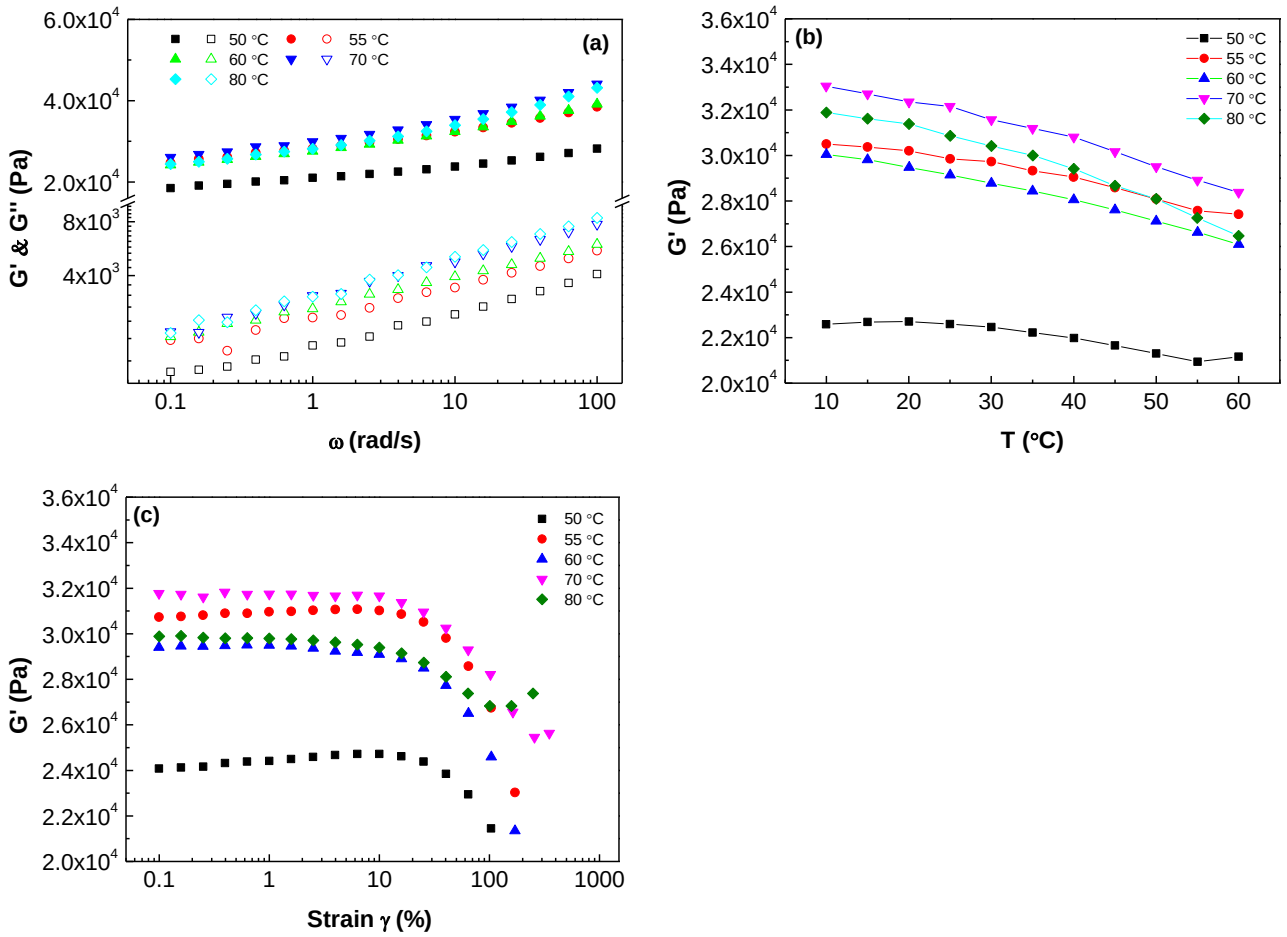

Fig. S3. (a) $G'(\omega)$ and $G''(\omega)$ as a function of frequency at $\gamma = 0.5\%$ and $T = 25$ ℃; (b) $G'(T)$ as a function of temperature at $\omega = 1$ rad/s and $\gamma = 0.5\%$; and (c) $G'(\gamma)$ as a function of strain amplitude γ at $\omega = 10$ rad/s and $T = 60$ ℃, measured for samples with different reaction temperatures (T_r).

3 Tables

Table S1. Effect of crosslinker concentration ($\%C$) on the rheokinetic parameters obtained by curve fitting using Equation 1[(a)]

$\%C$ (%)	G'_∞ (Pa)	θ (s)	n	P (Pa/s)
0.00	21692 (1294)[(b)]	769 (51)	1.96 (0.05)	11.61 (0.31)
0.05	26558 (877)	890 (27)	1.70 (0.05)	11.04 (0.56)
0.14	28642 (946)	838 (72)	2.21 (0.13)	16.77 (2.49)
0.28	38635 (1205)	753 (15)	2.31 (0.05)	27.06 (0.88)
0.41	41877 (970)	791 (42)	2.48 (0.12)	30.16 (1.27)
0.55	49813 (611)	706 (21)	2.38 (0.08)	39.15 (0.71)
Regression models:	$G'_\infty = 23002 + 48547 \times \%C,\ R^2 = 0.987$			
	$P = 10.97 + 50.91 \times \%C,\ R^2 = 0.976$			

(a) NCS was used with $T_r = 60$ ℃, $\%I = 0.36\%$.

(b) Standard deviations for triplicate measurements are given in parentheses.

Table S2. Effect of initiator concentration (*%I*) on the rheokinetic parameters obtained by curve fitting using Equation 1[(a)]

%I (%)	G'_∞ (Pa)	θ (s)	n	P (Pa/s)
0.11	25435 (1224)[(b)]	1482 (83)	2.52 (0.19)	9.32 (0.19)
0.21	27628 (881)	1021 (22)	2.31 (0.05)	13.67 (0.55)
0.36	28642 (946)	838 (72)	2.21 (0.13)	16.77 (2.49)
0.71	27339 (1037)	548 (22)	1.88 (0.05)	20.51 (0.49)
1.42	28511 (370)	363 (13)	1.34 (0.03)	23.23 (1.42)
Regression models:	$\theta = 444 \times (\%I)^{-0.54},\ R^2 = 0.997$			
	$n = 2.47 - 0.80 \times \%I,\ R^2 = 0.997$			
	$P = 21.97 - 19.40 \times 0.02^{(\%I)},\ R^2 = 0.995$			

(a) NCS was used with $T_r = 60$ ℃, $\%C = 0.05\%$.

(b) Standard deviations for triplicate measurements are given in parentheses.

Table S3. Effect of reaction temperature (T_r) on the rheokinetic parameters obtained from the curve fitting of Equation 1[(a)]

T_r (°C)	G'_∞ (Pa)	G'_∞ (T = 25 °C)	θ (s)	n	P (Pa/s)
50	25814 (2144)[(b)]	21798 (793)	2657 (262)	2.47 (0.14)	5.18 (0.15)
55	26371 (224)	29025 (826)	1415(75)	2.61 (0.06)	10.54 (0.24)
60	26558 (877)	28359 (788)	890 (27)	1.70 (0.05)	11.04 (0.56)
70	24611 (109)	31030 (1121)	429 (12)	1.72 (0.05)	22.59 (0.42)
80	23096 (1049)	29515 (1346)	297 (5)	1.18 (0.01)	20.23 (0.71)
Regression models:	$\theta = 245 + 1.23exp^{-1.23T_r},\ R^2 = 0.999$				

(a) NCS was used with $\%C = 0.05\%,\ \%I = 0.36\%$.

(b) Standard deviations for triplicate measurements are given in parentheses.

Table S4. Effect of amylose/amylopectin ratio on the rheokinetic parameters obtained from the curve fitting of Equation 1[(a)]

Type of starch	Amylose/amylopectin ratio	G'_∞ (Pa)	θ (s)	n	P (Pa/s)
WCS	0/100	9101 (429)[(b)]	747 (16)	2.07 (0.08)	6.28 (0.10)
NCS	27/73	26558 (877)	890 (27)	1.70 (0.05)	11.04 (0.56)
G50	50/50	90180 (1433)	814 (80)	2.55 (0.27)	54.93 (3.64)
G80	80/20	121518 (4211)	950 (75)	2.16 (0.19)	59.12 (5.35)

(a) $T_r = 60$ °C, $\%C = 0.05\%$, $\%I = 0.36\%$.

(b) Standard deviations for triplicate measurements are given in parentheses.

References

Qiao, D., Liu, H., Yu, L., Bao, X., Simon, G. P., Petinakis, E., et al. (2016). Preparation and characterization of slow-release fertilizer encapsulated by starch-based superabsorbent polymer. *Carbohydrate Polymers, 147*, 146-154.

Qiao, D., Yu, L., Bao, X., Zhang, B., & Jiang, F. (2017). Understanding the microstructure and absorption rate of starch-based superabsorbent polymers prepared under high starch concentration. *Carbohydrate Polymers, 175*, 141-148.

Zhang, Z., Chen, P., Du, X., Xue, Z., Chen, S., & Yang, B. (2014). Effects of amylose content on property and microstructure of starch-graft-sodium acrylate copolymers. *Carbohydrate Polymers, 102*, 453-459.

Zou, W., Yu, L., Liu, X., Chen, L., Zhang, X., Qiao, D., et al. (2012). Effects of amylose/amylopectin ratio on starch-based superabsorbent polymers. *Carbohydrate Polymers, 87*(2), 1583-1588.